Isogeometric Finite Elements With Surface Impedance Boundary Conditions

Rafael Vázquez[1], Annalisa Buffa[1], Luca Di Rienzo[2], and Dongwei Li[3]

[1]Istituto di Matematica Applicata e Tecnologie Informatiche del CNR, Pavia I-27100, Italy
[2]Dipartimento di Elettronica, Informazione e Bioingegneria, Politecnico di Milano, Milan I-20133, Italy
[3]ElectroScience Laboratory, Ohio State University, Columbus, OH 43212 USA

I. Introduction

ISOGEOMETRIC Analysis (IGA) [1] is a discretization technique, which was introduced to simplify the interaction between computer-aided design (CAD) software and numerical solvers. The discretization in IGA is done with Non-Uniform Rational B-Splines (NURBS), a family of functions that is widely used in CAD [2]. The main advantage of IGA with respect to standard FEM is that it uses a representation of the geometry in terms of NURBS, which is maintained during refinement. This is particularly interesting for the implementation of high-order surface impedance boundary conditions (SIBCs), because the curvature of a NURBS parametrization can be computed exactly at any point.

The use of NURBS together with SIBCs was already applied in [3], in that case using the BEM to discretize an integral equation for the computation of per-unit-length (p.u.l.) parameters of multiconductor transmission lines. In this paper, we present the variational formulation of the same 2-D problem in harmonic regime, and we solve it numerically with IGA. It is not our goal to compare the present method with the BEM proposed in [3], but to present an alternative discretization technique. As a matter of fact, the well-known advantages and drawbacks when comparing BEM and FEM (matrix sparsity, dimension of the computational domain, singular integrals, etc.) also apply when comparing the method in this paper with the NURBS-based BEM in [3].

The same problem was already discretized with FEM in [4]. With respect to that paper, our formulation: 1) applies the SIBC also to the conductors where the current is imposed; 2) includes high-order SIBCs; and 3) accurately takes into account the curvature with the use of NURBS.

Manuscript received June 24, 2013; revised August 9, 2013; accepted August 27, 2013. Date of current version February 21, 2014. Corresponding author: R. Vázquez (e-mail: vazquez@imati.cnr.it).

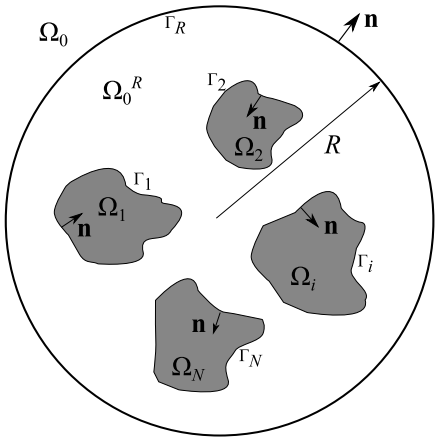

Fig. 1. Geometry of the problem.

II. Magnetic Vector Potential Formulation

Consider a set of N infinitely long parallel conductors, with cross sections Ω_i, $i = 1, \ldots, N$ (see Fig. 1). Each conductor is assumed to have electrical conductivity σ_i and magnetic permeability μ_i, with μ_0 the permeability of free space.

We consider the time-harmonic eddy-current model, with a 2-D formulation based on the magnetic vector potential $\mathbf{A} = A\mathbf{e}_z$, as in [5]. Splitting the potential into "source" and "eddy" components, $A = A^s + A^e$, it can be seen that A^s is constant in each conductor, and its value in Ω_i will be denoted by A^s_i. Then, in the 2-D formulation, the eddy component A^e satisfies the following equation in each conductor:

$$\nabla^2 A^e_{\text{int}} = \mathrm{j}\omega\mu_i\sigma_i A^e_{\text{int}} \qquad \text{in } \Omega_i \tag{1}$$

and in the nonconducting domain

$$\nabla^2 A^e_{\text{ext}} = 0 \qquad \text{in } \Omega_0. \tag{2}$$

Denoting by Γ_i the boundary of (the cross section of) each conductor, and by $\mathbf{n}$ the unit normal vector exterior to Ω_0, the equations for A^e are completed with interface conditions

on Γ_i

$$[A^e]_{\Gamma_i} = -A_i^s, \quad \left[\frac{1}{\mu}\frac{\partial A^e}{\partial \mathbf{n}}\right]_{\Gamma_i} = 0 \tag{3}$$

where the brackets denote the jump on the interface, $[A^e] = A^e_{\text{int}} - A^e_{\text{ext}}$. The problem is completed with a radiation condition that, in practice, is replaced by truncating the infinite domain at the boundary $\Gamma_R = \{(x, y) : x^2 + y^2 = R^2\}$, and applying the second-order absorbing boundary condition (see [6], Section 3.3)

$$\frac{\partial A^e_{\text{ext}}}{\partial \mathbf{n}} + \frac{3A^e_{\text{ext}}}{8R} - \frac{1}{2R}\frac{\partial^2 A^e_{\text{ext}}}{\partial \xi^2} = 0 \qquad \text{on } \Gamma_R \tag{4}$$

where ξ denotes the curvilinear coordinate over the boundary contour.

Since the source component A^s is unknown, a condition on the intensity flowing in each conductor is also needed

$$\int_{\Gamma_i} \frac{1}{\mu_0}\frac{\partial A^e_{\text{ext}}}{\partial \mathbf{n}} = I_i, \qquad i = 1, \ldots, N. \tag{5}$$

III. Surface Impedance Boundary Conditions

The general idea of applying SIBCs is to replace the solution of the problem inside the conductor given by (1), with an approximate boundary condition that replaces the field A^e_{int}. The method is valid under the condition of skin effect, that is, in each conductor the penetration depth $\delta_i = \sqrt{2/\omega\mu_i\sigma_i}$ is much smaller than the characteristic size of the conductor cross section.

Defining $\alpha = \sqrt{2\mathrm{j}}$, and using the interface conditions (3), the first-order (Leontovich) and second-order (Mitzner) SIBCs on Γ_i are [5], [7]

$$\frac{1}{\mu_0}\frac{\partial A^e_{\text{ext}}}{\partial \mathbf{n}} = \frac{-\alpha}{\mu_i\delta_i}(A^e_{\text{ext}} - A^s_i) \tag{6}$$

$$\frac{1}{\mu_0}\frac{\partial A^e_{\text{ext}}}{\partial \mathbf{n}} = \frac{-2\alpha^2}{\mu_i(\delta_i^2 c + 2\alpha\delta_i)}(A^e_{\text{ext}} - A^s_i) \tag{7}$$

where $c = c(\xi)$ is the (signed) curvature of the contour of the cross section.

IV. Weak Formulation

The weak formulation of the problem is obtained from (2) divided by μ_0. Multiplying by a test function v, and applying the absorbing boundary condition (4) and the SIBCs (6), we get

$$\frac{1}{\mu_0}\left(\int_{\Omega_0^R} \nabla A^e_{\text{ext}} \cdot \nabla v \,\mathrm{d}S + \frac{1}{2R}\int_{\Gamma_R} \frac{\partial A^e_{\text{ext}}}{\partial \xi}\frac{\partial v}{\partial \xi}\,\mathrm{d}\xi + \frac{3}{8R}\int_{\Gamma_R} A^e_{\text{ext}} v \,\mathrm{d}\xi\right) + \sum_{i=1}^{N}\int_{\Gamma_i} \frac{\alpha}{\mu_i\delta_i}(A^e_{\text{ext}} - A^s_i) v \, d\xi = 0. \tag{8}$$

Instead, if we apply the SIBC (7), we obtain

$$\frac{1}{\mu_0}\left(\int_{\Omega_0^R} \nabla A^e_{\text{ext}} \cdot \nabla v \,\mathrm{d}S + \frac{1}{2R}\int_{\Gamma_R} \frac{\partial A^e_{\text{ext}}}{\partial \xi}\frac{\partial v}{\partial \xi}\,\mathrm{d}\xi + \frac{3}{8R}\int_{\Gamma_R} A^e_{\text{ext}} v \,\mathrm{d}\xi\right) + \sum_{i=1}^{N}\int_{\Gamma_i} \frac{2\alpha^2(A^e_{\text{ext}} - A^s_i)}{\mu_i(\delta_i^2 c + 2\alpha\delta_i)} v \,\mathrm{d}\xi = 0. \tag{9}$$

Since the constants A^s_i are also unknown, in order to discretize the problem with Galerkin's method the SIBCs must also be applied to the intensity equation (5). Applying condition (6) this becomes

$$\int_{\Gamma_i} \frac{\alpha}{\mu_i\delta_i}(A^e_{\text{ext}} - A^s_i)\,\mathrm{d}\xi = I_i, \qquad i = 1, \ldots, N \tag{10}$$

and applying condition (7), we get

$$\int_{\Gamma_i} \frac{2\alpha^2(A^e_{\text{ext}} - A^s_i)}{\mu_i(\delta_i^2 c + 2\alpha\delta_i)}\,\mathrm{d}\xi = I_i, \qquad i = 1, \ldots, N. \tag{11}$$

Hence, the variational problem for Leontovich's condition is given by (8) and (10). For Mitzner's condition, it is given by (9) and (11). These weak formulations can be discretized with the finite element method. In this paper, we discretize them with an isogeometric method, that we describe in the following section.

V. NURBS and Isogeometric Analysis

From an ordered knot vector $\Xi = \{0 = \zeta_1, \ldots, \zeta_{n+p+1} = 1\}$, n univariate B-spline basis functions of degree p are computed using the Cox-De Boor recursive formula

$$\mathsf{B}_{k,0}(\zeta) = \begin{cases} 1, & \text{if } \zeta_k \le \zeta < \zeta_{k+1} \\ 0, & \text{otherwise} \end{cases}$$

$$\mathsf{B}_{k,p}(\zeta) = \frac{\zeta - \zeta_k}{\zeta_{k+p} - \zeta_k}\mathsf{B}_{k,p-1}(\zeta) + \frac{\zeta_{k+p+1} - \zeta}{\zeta_{k+p+1} - \zeta_{k+1}}\mathsf{B}_{k+1,p-1}(\zeta).$$

These B-splines form a basis of the space of piecewise polynomials of degree p, with the number of continuous derivatives on each knot ranging from 0 up to $p-1$, depending on the multiplicity of the knot. B-spline basis functions are positive and locally supported.

Bivariate B-splines of degree (p, q) are simply defined from the previous formula using tensor products. Bivariate NURBS basis functions are defined as rational B-splines by associating a positive weight to each B-spline function, in the form

$$\hat{N}_{k_1,k_2}(\boldsymbol{\zeta}) = \frac{w_{k_1,k_2} B_{k_1,p}(\zeta_1),\, B_{k_2,q}(\zeta_2)}{\sum_{j_1=1}^{n}\sum_{j_2=1}^{m} w_{j_1,j_2} B_{j_1,p}(\zeta_1),\, B_{j_2,q}(\zeta_2)}$$

defined for $\boldsymbol{\zeta} = (\zeta_1, \zeta_2)$ in the unit square. A NURBS surface is then constructed as the image of the unit square by a certain parametrization $\mathbf{F}$, which is given by a linear combination of NURBS basis functions, associating a control point $\mathbf{C}_{k_1,k_2}$ to each basis function, in the form (see [2])

$$\mathbf{F}(\boldsymbol{\zeta}) := \sum_{k_1=1}^{n}\sum_{k_2=1}^{m} \hat{N}_{k_1,k_2}(\boldsymbol{\zeta})\mathbf{C}_{k_1,k_2}. \tag{12}$$

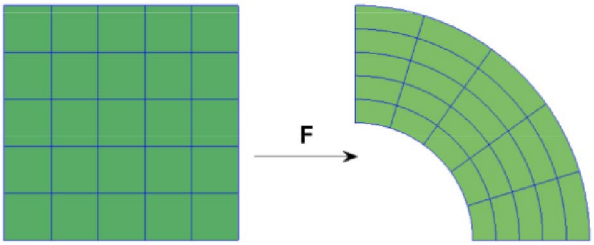

Fig. 2. Partition of the unit square given by the knot vectors, and the partition induced in the physical domain through the parametrization $\mathbf{F}$.

We note that the algorithms of knot insertion and degree elevation, explained in [2], allow to recompute the control points after inserting new knots in the knot vector or raising the degree, respectively, to maintain the same parametrization (12).

For the discretization of the weak formulation introduced in the previous section we use IGA [1], a numerical technique which is based on NURBS. Assuming that the domain Ω_0 is given as a NURBS geometry, like in (12), and invoking the isoparametric concept, the same space of NURBS functions is used for the discretization of the field A^e_{ext}, which takes the form

$$A^e_{\text{ext}} = \sum_{k_1,k_2=1}^{n,m} A_{k_1,k_2} N_{k_1,k_2}$$

with the basis functions in the physical domain defined by

$$N_{k_1,k_2}(\mathbf{x}) = \hat{N}_{k_1,k_2}\left(\mathbf{F}^{-1}(\mathbf{x})\right).$$

The implementation of IGA is very similar to that of FEM, the main differences appearing in the assembly of the matrix of the linear system. In practice, the knot vectors used to define the geometry generate a partition in the unit square, and through the parametrization $\mathbf{F}$, a partition of the physical domain, as shown in Fig. 2. To assemble the matrix, the integrals on each element are computed numerically using standard Gaussian quadrature rules. The basis functions and the parametrization $\mathbf{F}$, and also their derivatives, can be evaluated at the quadrature points using the algorithms for NURBS explained in [2]. A possible alternative is to evaluate the functions using Bézier extraction, as proposed in [8]. For more details on the implementation of IGA, we refer to [1] and [9].

One of the main features of IGA is that, once the parametrization (12) is given, refinement can be done automatically using the algorithms of knot insertion and degree elevation. In fact, these two algorithms are the analogous of h-refinement and p-refinement in FEM [1]. Moreover, a combination of both allows the so-called k-refinement, which consists of raising the degree and the continuity at the same time. This gives more smooth solutions than the ones computed by FEM, since NURBS basis functions of degree p have up to $p-1$ continuous derivatives.

There is numerical evidence that the higher continuity of NURBS functions leads to better convergence in terms of degrees of freedom with respect to FEM. However, it has been recently shown that the computational cost per degree of freedom is also increased, both in the assembly of the matrix and in the solution of the linear system [10]. The study of efficient quadrature rules for splines and NURBS [11], and the development of efficient solvers and preconditioners are two active research topics for IGA methods.

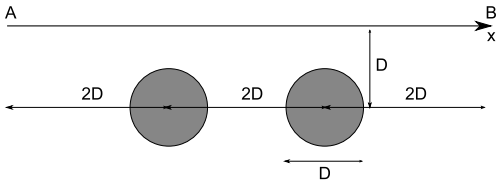

Fig. 3. Geometry of two parallel conductors. $D = 2$ mm.

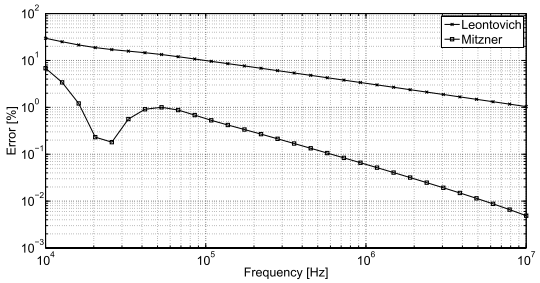

Fig. 4. Relative error in p.u.l. resistance for two circular copper cables of diameter 2 mm. Distance between the centers of the conductors is 4 mm.

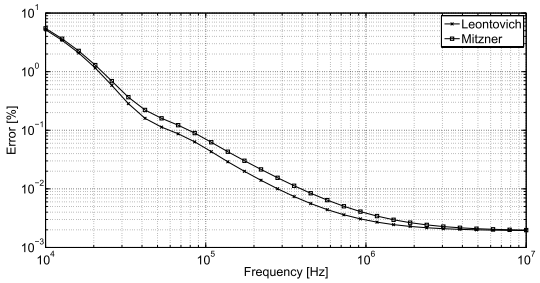

Fig. 5. Relative error in p.u.l. inductance for two circular copper cables of diameter 2 mm. Distance between the centers of the conductors is 4 mm.

VI. Numerical Results

The implementation is validated by solving the canonical case of two parallel circular copper conductors, with conductivity $\sigma = 5.8 \times 10^7$ S/m. The diameter of each conductor is 2 mm, and the distance between their centers is 4 mm, as shown in Fig. 3. With the numerical solution, we have computed the p.u.l. resistance and inductance, following the procedure described in [5] and comparing numerical results with the analytical solution [12]. The relative errors, shown in Figs. 4 and 5 converge to zero when frequency goes to infinity. In particular, Fig. 4 shows the higher order convergence of the Miztner approximation compared to Leontovich approximation, as predicted by the theory, which states that the approximation of the kth order is $O(\delta^{k+1})$. The applied discretization is with NURBS of degree 3, the number of elements is equal to 72 900 and the number of degrees of freedom is equal to 76 911. The radius of the external boundary is $R = 240$ mm. Our IGA results are very close to those obtained with the BEM formulation in [3], showing that they are due to the chosen SIBC and do not depend on the discretization technique. Fig. 6 shows the impact of the domain size on the accuracy of the inductance: as it can be noted the

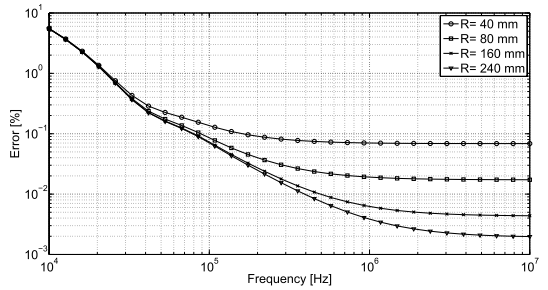

Fig. 6. Relative error in p.u.l. inductance in the Mitzner approximation for different values of the radius R of the computational domain.

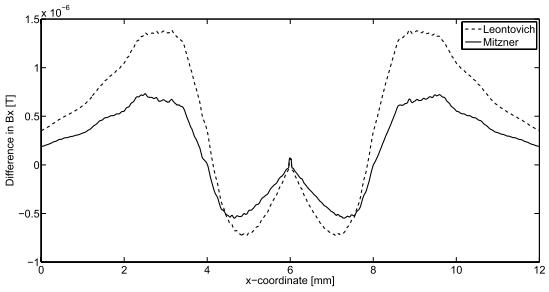

Fig. 7. Absolute error of $|B_x|$ along the line AB in Fig. 3, with respect to the FEM simulation.

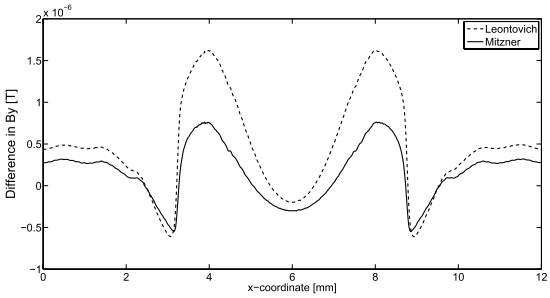

Fig. 8. Absolute error of $|B_y|$ along the line AB in Fig. 3, with respect to the FEM simulation.

error does not go below a threshold, which becomes lower increasing the radius of the computational domain. This is because the computation of the inductance from the variational formulation is equivalent to computing the magnetic energy in the truncated domain, but the real value should take into account the whole space. This could be overcomed with the use of infinite elements, for instance, but it is beyond the scope of this paper.

In order to show the gain in accuracy when computing the magnetic field near the conductors, the magnitudes of the x- and y-components of the magnetic field are calculated on the line A–B represented in Fig. 3 at 10 kHz, by means of IGA formulations with first- and second-order SIBCs, and compared with those obtained using a commercial FEM code [13]. As can be noted in Figs. 7 and 8, Mitzner's SIBC provides better accuracy with respect to Leontovich's SIBC over the line.

VII. Conclusion

The implementation of Leontovich's and Mitzner's surface impedance boundary conditions with isogeometric finite elements is tested in the simple canonical case of two circular parallel conductors, showing the higher order convergence of the latter. The exact computation of the curvature provided by NURBS opens the way to variational formulations including higher order impedance boundary conditions of Rytov's kind. Even if more complicated examples are needed to show the benefits of the proposed formulation, preliminary results are promising and in good agreement with those obtained with boundary elements, with and without the use of NURBS. The extension to the 3-D case would require the use of the SIBCs studied in [14] and the isogeometric elements in [15].

Acknowledgment

The work of A. Buffa and R. Vázquez has been partially supported by the European Research Council through the FP7 Ideas Starting Grant 205004: GeoPDEs–Innovative compatible discretization techniques for Partial Differential Equations.

References

[1] J. A. Cottrell, T. J. R. Hughes, and Y. Bazilevs, *Isogeometric Analysis: Toward Integration of CAD and FEA*. New York, NY, USA: Wiley, 2009.

[2] L. Piegl and W. Tiller, *The Nurbs Book*. New York, NY, USA: Springer-Verlag, 1997.

[3] R. Vázquez, A. Buffa, and L. Di Rienzo, "NURBS-based BEM implementation of high-order surface impedance boundary conditions," *IEEE Trans. Magn.*, vol. 48, no. 12, pp. 4757–4766, Dec. 2012.

[4] A. Darcherif, A. Raizer, J. Sakellaris, and G. Meunier, "On the use of the surface impedance concept in shielded and multiconductor cable characterization by the finite element method," *IEEE Trans. Magn.*, vol. 28, no. 2, pp. 1446–1449, Mar. 1992.

[5] L. Di Rienzo, S. Yuferev, and N. Ida, "Computation of the impedance matrix of multiconductor transmission lines using high-order surface impedance boundary conditions," *IEEE Trans. Electromagn. Compat.*, vol. 50, no. 4, pp. 974–984, Nov. 2008.

[6] F. Ihlenburg, *Finite Element Analysis of Acoustic Scattering* (Applied Mathematical Sciences), vol. 132. New York, NY, USA: Springer-Verlag, 1998.

[7] H. Haddar, P. Joly, and H.-M. Nguyen, "Generalized impedance boundary conditions for scattering by strongly absorbing obstacles: The scalar case," *Math. Models Methods Appl. Sci.*, vol. 15, no. 8, pp. 1273–1300, 2005.

[8] M. J. Borden, M. A. Scott, J. A. Evans, and T. J. R. Hughes, "Isogeometric finite element data structures based on Bézier extraction of NURBS," *Int. J. Numer. Methods Eng.*, vol. 87, nos. 1–5, pp. 15–47, Aug. 2010.

[9] C. de Falco, A. Reali, and R. Vázquez, "GeoPDEs: A research tool for isogeometric analysis of PDEs," *Adv. Eng. Softw.*, vol. 42, no. 12, pp. 1020–1034, Dec. 2011.

[10] N. Collier, D. Pardo, L. Dalcin, M. Paszynski, and V. Calo, "The cost of continuity: A study of the performance of isogeometric finite elements using direct solvers," *Comput. Methods Appl. Mech. Eng.*, vols. 213–216, pp. 353–361, Mar. 2012.

[11] F. Auricchio, F. Calabrò, T. Hughes, A. Reali, and G. Sangalli, "A simple algorithm for obtaining nearly optimal quadrature rules for NURBS-based isogeometric analysis," *Comput. Methods Appl. Mech. Eng.*, vols. 249–252, pp. 15–27, Jan. 2012.

[12] V. Belevitch, "Theory of the proximity effect in multiwire cables—Part I," *Philips Res. Rep.*, vol. 32, no. 1, pp. 16–43, 1977.

[13] (2011, Apr.). *ANSYS Maxwell 2D V.13* [Online]. Available: http://www.ansoft.com

[14] H. Haddar, P. Joly, and H.-M. Nguyen, "Generalized impedance boundary conditions for scattering problems from strongly absorbing obstacles: The case of Maxwell's equations," *Math. Models Methods Appl. Sci.*, vol. 18, no. 10, pp. 1787–1827, Oct. 2008.

[15] A. Buffa, J. Rivas, G. Sangalli, and R. Vázquez, "Isogeometric discrete differential forms in three dimensions," *SIAM J. Numer. Anal.*, vol. 49, no. 2, pp. 818–844, Apr. 2011.